International Journal of Bio-Inorganic Hybrid Nanomaterials

The Study of Pure and Mn Doped ZnO Nanocrystals for Gas-sensing Applications

Meysam Mazhdi[1*], Jabar Saydi[1, 2], Faezeh Mazhdi[3]

[1] *M.Sc., Department of Physics, Faculty of Sciences, I.H.U, Tehran, Iran*
[2] *Ph.D. Student, Department of Physics, Faculty of Sciences, Young Research Club, Islamic Azad University of East Branch, Tehran, Iran*
[3] *B.Sc., Department of Electrical and Robotics Engineering, University of Shahrood Technology, Shahrood, Iran*

ABSTRACT

ZnO and ZnO: Mn nanocrystals were synthesized via reverse micelle method. The structural properties of nanocrystals were investigated by XRD. The XRD results indicated that the synthesized nanocrystals had a pure wurtzite (hexagonal phase) structure. Resistive gas sensors were fabricated by providing ohmic contacts on the tablet obtained from compressed nano-crystals powder and the installation of a custom made micro heater beneath the substrate. Sensitivity (S= Ra/Rg) of ZnO and ZnO: Mn nanocrystals were investigated as a function of temperature and concentration of ethanol and gasoline vapor. The obtained data indicated that optimum working temperatures of the ZnO and ZnO: Mn nanocrystals sensors are about 360°C and 347°C for ethanol vapor and about 287°C and 335°C for gasoline vapor. Based on gas sensing results, although Mn impurity reduces the Sensitivity but the sensor got saturated at much higher gas concentration.

Keyword: ZnO Nanocrystals; Gas sensor; Response time; Recovery time; Micelle method.

1. INTRODUCTION

Semiconductor nanocrystals have attracted great application during the past two decades. Compared with the corresponding bulk materials, new devices from semiconductor nanocrystals may possess novel optical and electronic properties, which are potentially useful for technological applications, [1-3]. Extremely high surface area to volume ratio can be obtained with the decrease of particle size,

which leads to an increase in surface specific active sites for chemical reactions and photon absorptions. The enhanced surface area also affects chemical reaction dynamics. The size quantization increases the energy band gap between the conduction band electrons and valence band holes which leads to change in their optical properties [3]. Zinc oxide, a typical II-VI compounding semiconductor, with a

(*) Corresponding Author - e-mail: meisam.physics@gmail.com

Int. J. Bio-Inorg. Hybd. Nanomat., Vol. 2, No. 1 (2013), 295-302

Mazhdi M et al

direct band gap of 3.2 eV at room temperature and 60 meV as excitonic binding energy, is a very good luminescent material used in displays, ultraviolet and visible lasers, solar cells components, gas sensors and varistors [1, 2]. Recently, a number of techniques such as reverse micelle, hydrothermal, sol-gel, and wet chemical have been employed in the synthesis of zinc oxide nanocrystals [1-4]. However, the reverse micelle technique is one of the more widely recognized methods due to its advantages, for instance, soft chemistry, demanding no extreme pressure or temperature control, easy to handle, and requiring no special or expensive equipment [4].

In current material science research, the use of nano sized materials for gas sensors is rapidly arousing interest in the scientific community. One reason is that the surface to bulk ratio for the nano sized materials is much greater than those for coarse materials. As another reason, the conduction type of the material is determined by the grain size of the material. When the grain size is small enough (the actual grain size D is less than twice the space-charge depth L), the material resistivity is determined by grain control, and the material conduction type becomes surface conduction type [5]. Hence, the grainsize reduction is one of the main factors in enhancing the gas sensing properties of semiconducting oxides.

In this scientific work, ZnO and ZnO: Mn nanocrystals were synthesized through the reverse micelle method. The structural characteristics of these nanocrystals were analyzed. The sensitivity of the fabricated nanocrystals to gasoline and ethanol vapor contamination was measured. The results indicated a profound increase in the gas sensitivity due to nanocrystalline nature of the sensors.

2. EXPERIMENTAL

2.1. Materials
ZnO and ZnO: Mn nanocrystals were fabricated through the mixture of two equal microemulsion systems. In micro emulsion I, butanol, PVP and aqueous solution of zinc acetate (0.1 molar ratios)

with the molar ratio of 1:1:0.4 was used as oil, surfactant and aqueous phase. Microemulsion II had similar ingredients but instead of aqueous solution, a solution of potassium hydroxide and water was used as aqueous media. Both micro emulsion solutions I and II were mixed vigorously with a magnetic stirrer. After centrifugation, ZnO and Mn doped ZnO precipitates were collected and were dried at 250°C for 3 hours [3, 4]. The nanocrystals were compressed as tablets and were annealed at 500°C for 2 hours by using a temperature controlled heating element. The tablets were used as gas sensor. The system employed is schematically shown in Figure 1.
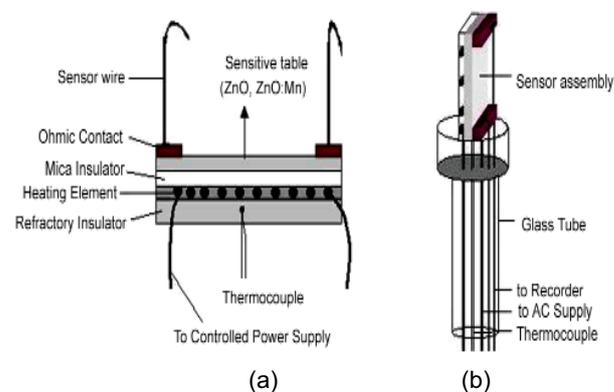
Figure 1: Schematic illustrations of the fabricated gas sensor (a) and the sensor probe (b).

2.2. Sensor fabrication and measurements
The produced tablet annealing temperature was kept at 500°C for 2 hours by using a temperature controlled heating element. Therefore we use the tablet as a gas sensor. Ohmic connections are used in order to create relation between sensor and electric circuit that has been shown in Figure 2. These connections contact through platinum wire and paste. The used paste kind is similar to tablet. The sample was then attached to a temperature-controlled micro-heater, and was mounted on a refractory stand, so that the temperature of the sample could be adjusted in the 160-430°C temperature range. The structure of the device is schematically presented in Figure 1 (a). A sensor probe was formed by mounting the sample on an insulated layer through which two insulated

Mazhdi M et al

Int. J. Bio-Inorg. Hybd. Nanomat., Vol. 2, No. 1 (2013), 295-302

connection cables were guided to the temperature control unit and the impedance measurement device respectively. For each sensitivity measurement, the sensor probe was set at the desired operating temperature and a 10 min time was allowed for the probe temperature to stabilize. Then, a constant AC voltage (4 v, 80 Hz) was applied to the sensor, while the current passing through the device was recorded. DC fields could cause ionic migration and electrode instability which were of much lesser concern in the case of AC voltages applied. The sensitivity measurement was then achieved by the insertion of the probe into a 1.5 Lit glass tank containing air with a predetermined contamination (in this work, gasoline and ethanol) level. To avoid errors caused by condensation of the contaminating gas on the walls of the tank, it was externally heated.
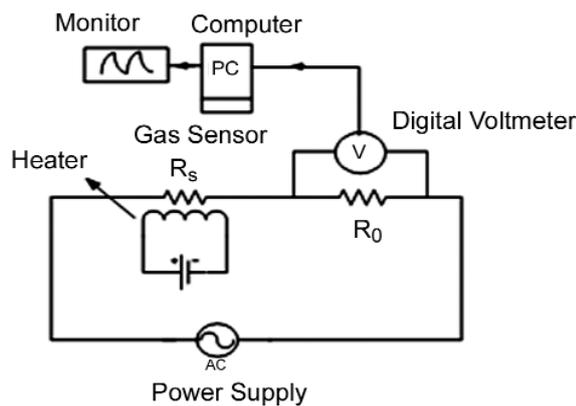

Figure 2: *Gas sensor Electric circuit.*

2.3. Characterization
Obtained nanocrystals were analyzed by X-ray diffractometer (Scifert, 3003 TT) with Cu-k$_\alpha$ radiation, Atomic absorption spectrometer (PERKIN ELMER, 1100 B) and sensitivity of these nanocrystals investigated by resistive gas sensors for ethanol and gasoline vapor.

3. RESULTS AND DISCUSSION

3.1. XRD analysis
Figure 3 shows the XRD patterns of ZnO and ZnO: Mn nanocrystals. The spectrums show three broad peaks for ZnO and ZnO: Mn at the 2θ= 31.744, 34.398, 36.223 and 2θ= 31.647, 34.313, and 36.131 positions. The three diffraction peaks correspond to the (100), (002), and (101) crystalline planes of hexagonal ZnO. All the peaks in the XRD patterns of ZnO and ZnO: Mn samples could be fitted with the hexagonal wurtzite structure having slightly increased lattice parameter values for Mn doped sample (For ZnO Nanocrystals *a*= 3.250 A°, *c*= 5.207 A° and ZnO: Mn nanocrystals, *a*= 3.256 A°, *c*= 5.212 A°) in comparison to that of pristine ZnO sample (*a*= 3.249A°, *c*= 5.205A°, JCPDS no. 36-1451). The increased lattice parameter values of Mn doped ZnO indicates the incorporation of manganese at zinc sites [4].
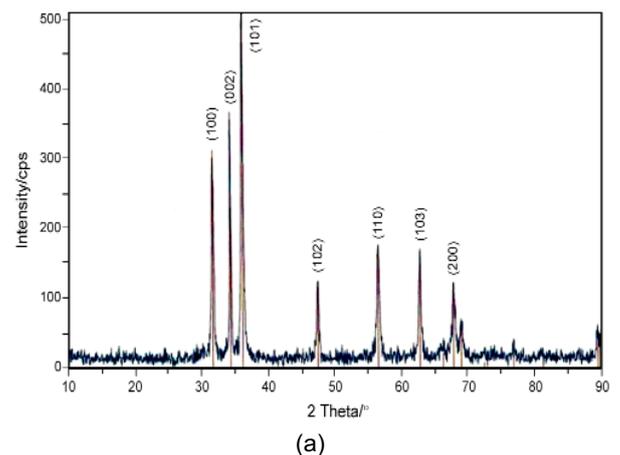
(a)
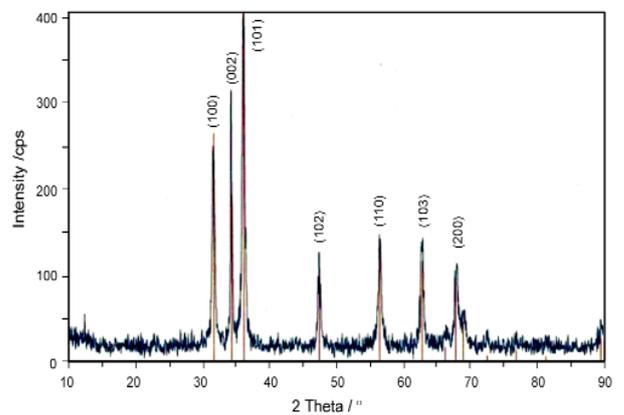
(b)

Figure 3: *XRD patterns of ZnO (a) and ZnO: Mn (b) nanocrystals.*

Int. J. Bio-Inorg. Hybd. Nanomat., Vol. 2, No. 1 (2013), 295-302

Mazhdi M et al

The broadening of the XRD lines is attributed to the nanocrystalline characteristics of the samples, which indicates that the particle size is in nano-meter range.

Inter planar spacing (d) is evaluated using the relation (1):

$$\frac{1}{d^2} = \frac{4}{3}\left(\frac{h^2 + hk + k^2}{a^2}\right) + \frac{l^2}{c^2} \tag{1}$$

D-spacing for (100), (002), and (101) planes are 2.8146, 2.6035, 2.4760 A° and 2.8204, 2.6062, 2.4806 A° for ZnO and ZnO: Mn nanocrystals, respectively. But, due to the size effect, the XRD peaks are broad. From the width of the XRD peak broadening, the mean crystalline size has been calculated using Scherer's equation [6]:

$$D = \frac{K\lambda}{\beta \cos\theta} \tag{2}$$

Where D is the diameter of the particle, K is a geometric factor taken to be 0.9, λ is the X-ray wavelength, θ is the diffraction angle and β is the full width at half maximum of the diffraction main peak at 2θ. The mean crystal size of ZnO and ZnO: Mn nanocrystals resulted to be 21 and 18 nm.

Also, we used the Williamson-Hall equation to calculate the strain and particle size of the samples. The Williamson-Hall equation is expressed as follows [6]:

$$\beta \cos\theta = \frac{k\lambda}{D} + 4\varepsilon \sin\theta \tag{3}$$

In this equation, $\beta\cos\theta$ is plotted against $\sin\theta$. Using a linear extrapolation to this plot, the intercept gives the particle size $k\lambda/D$ and the slope represents the strain (ε) for ZnO and ZnO: Mn nanoparticles. The size value and internal lattice strain value were found to be 23 and 21nm and 1.46×10^{-3} and 1.41×10^{-3} for ZnO and ZnO: Mn nanoparticles, respectively [3].

3.2. Atomic absorption study
The atomic absorption studies confirmed attendance of manganese at Zinc sites in ZnO: Mn nanocrystals. It supported the result obtained by XRD analysis. The amount of Mn doping is about 1% by weight.

3.3. TEM studies
TEM high magnification imaging allows the determination of size and individual crystallite morphology. TEM micrographs of the ZnO powder and size distribution histogram of nanocrystals obtained by TEM micrograph is presented in Figure 4. The main products are the spherical or quasi spherical nanocrystals and the average crystal size is related to 18-23 nm.

3.4. Sensitivity study
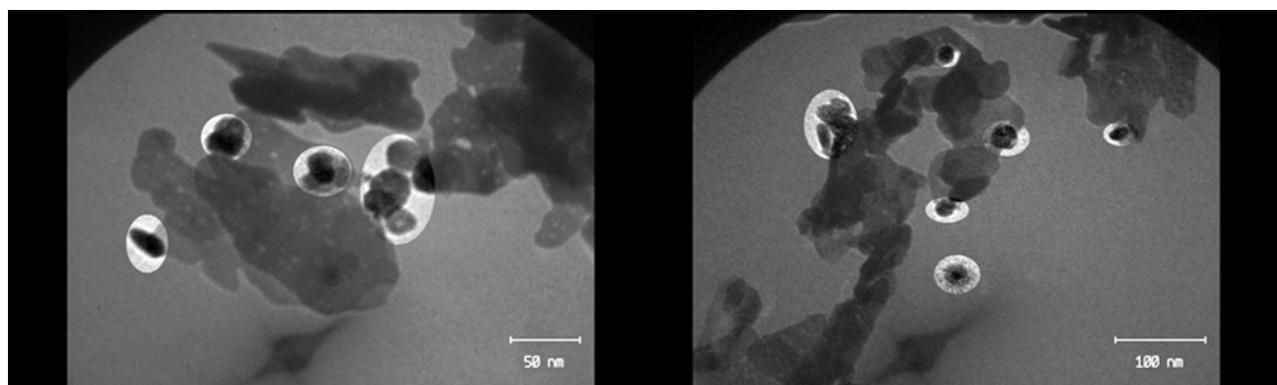Figure 2 shows schematic of resistance gas sensor

Figure 4: *TEM micrograph at high magnification and size distribution histogram of ZnO nanocrystals*.

that used in this experimental work. Sensor resistance R_s and constant resistance R_0 are connected continuously via power supply (V_c= 4 volts) and signal generator (80 Hz). Voltage loss V_0 of R_0, determine sensor conductivity changes in the presence of purpose gas and without it. Sensor resistance (R_s) obtains by the relation (4). R_0, V_0 and Vc are circuit resistance, voltage loss of R_0 and power supply voltage respectively.

$$R_s = \left(\frac{V_c}{V_0} - 1 \right) R_0 \qquad (4)$$

Sensor sensitivity for reducer gases defines as relative of sensor electric resistance in air to sensor electric resistance in presence of reducer gas:
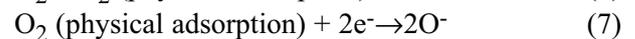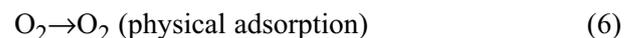
$$S = \frac{R_a}{R_g} \qquad (5)$$

The duration between the states that external voltage last until from the lowest value (i.e. in the presence of air) arrives to 90 % of highest value (i.e. in the presence of reducer gas) is called response time and restore time define as duration between the states that external voltage (by elimination of reducer gas) last until from the highest value arrives to 10 % of the lowest value [7, 8]. Semiconductor materials in ordinary temperature and pressure conditions almost are of electric insulator but when they are under the heat, their conductivity increase gradually. Figure 5 shows conductivity logarithmic graph (Arrhenius graph) of pure and doped zinc oxide and it indicates that increase in temperature lead to increase in conductivity.

In surface conduction sensors change in conduction resulted from reactions that occur in the semiconductor surface. In the presence of air and low temperatures, oxygen molecules adsorb on the surface of sensor physically. At the temperature between 240- 420°C, there is O^{2-} or O^- species on the surface of sensor that O^- is more stability and in high temperature dominant species is O^{2-} [9]. The reactions on surface of sensor are as:
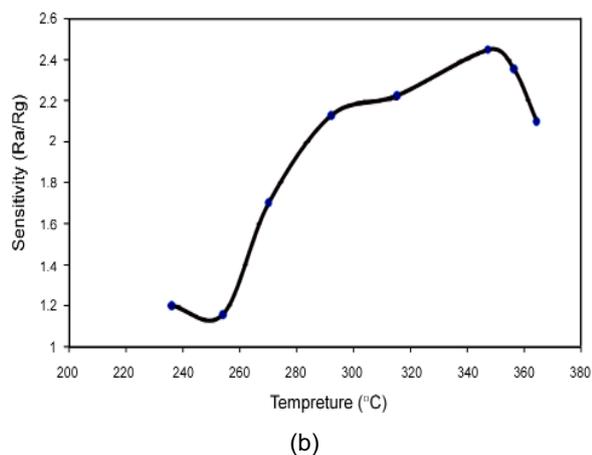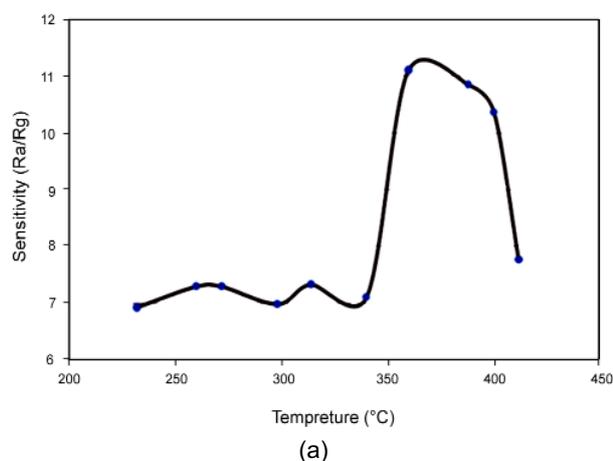

(a)

(b)
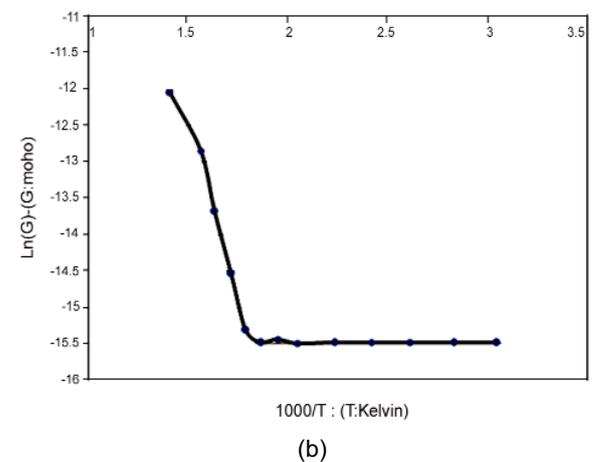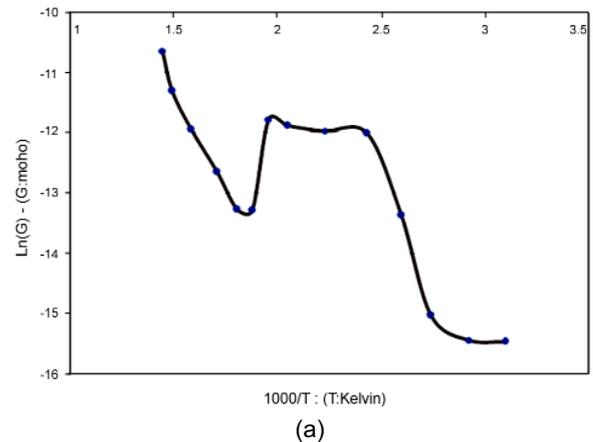
Figure 5: *Conductivity logarithmic graphs (Arrhenius graph) in the presence of air for ZnO (a), ZnO: Mn (b) nanocrystals.*

$$O_2 \rightarrow O_2 \text{ (physical adsorption)} \qquad (6)$$
$$O_2 \text{ (physical adsorption)} + 2e^- \rightarrow 2O^- \qquad (7)$$
$$O^- + e^- \rightarrow O^{2-} \qquad (8)$$

Oxygen vacancies in ZnO, acts as electron donors and also makes it an ntype semiconductor. Oxygen molecules in the ambient are adsorbed at the grain boundaries, which capture electrons from the conduction band and forming adsorbed oxygen ion. This causes a decrease in carrier concentration and increase in resistance of the sample. When the sensor is exposed to a reducing gas (in this work, ethanol and gasoline vapor), it reacts with the adsorbed oxygen and resulting in the release of the trapped electrons, come back into the conduction

Int. J. Bio-Inorg. Hybd. Nanomat., Vol. 2, No. 1 (2013), 295-302

Mazhdi M et al

band. This leads to an increase in carrier concentration and decrease in the resistance of the sensor. The properties of the sensors such as sensitivity, response and recovery times are known that to be temperature dependent.
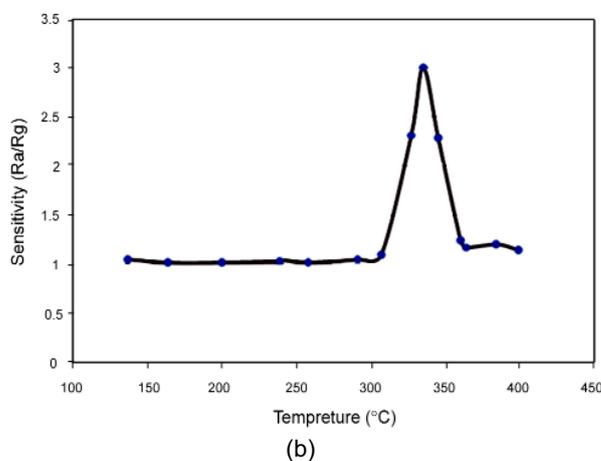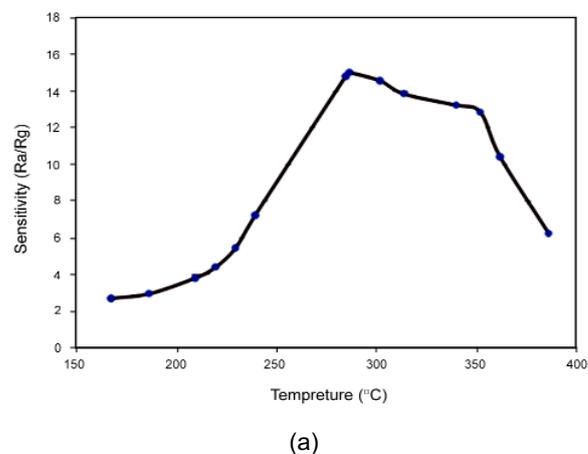
Sensitivity versus temperature for 1000 ppm of ethanol and gasoline vapor as a function of temperature is shown in Figures 6, 7. The temperature that sensor sensitivity arrives to maximum value defines as optimum working temperature (i.e. peak of Figures 6, 7).

respectively. Response and recovery times to ethanol vapor in working temperature of sensor for pure zinc oxide nanocrystals sensor are 5 and 80 seconds and also for zinc oxide nanocrystals doped by manganese are 19 and 13 seconds respectively. Response and recovery times to gasoline vapor in working temperature of sensor for pure zinc oxide nanocrystals sensor, 20 and 225 seconds and alsofor zinc oxide nanocrystals doped by manganese, 5 and 3 seconds have obtained respectively.

(a)

(b)

**Figure 6:** *Sensitivity versus temperature for 1000 ppm of ethanol vapor; ZnO (a), ZnO: Mn (b) nanocrystals.*

Optimum working temperature to ethanol vapor for pure and doped zinc oxide nanocrystals sample is 362°C and 345°C (Figure 6 a, b) and also for gasoline vapor is 285°C and 333°C (Figure 7 a, b)

(a)

(b)

Figure 7: *Sensitivity versus temperature for 1000 ppm of gasoline vapor; ZnO (a), ZnO: Mn (b) nanocrystals.*
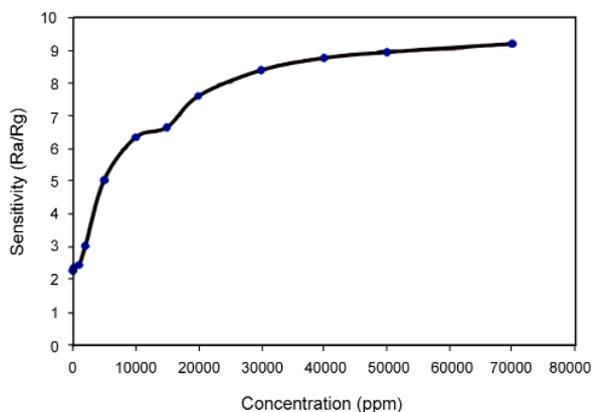
In this case study, we also investigated response of sensors to different concentration that has shown in Figures 8, 9. Increase of ethanol and gasoline vapor concentration lead to increase in nanocrystals sensing response.
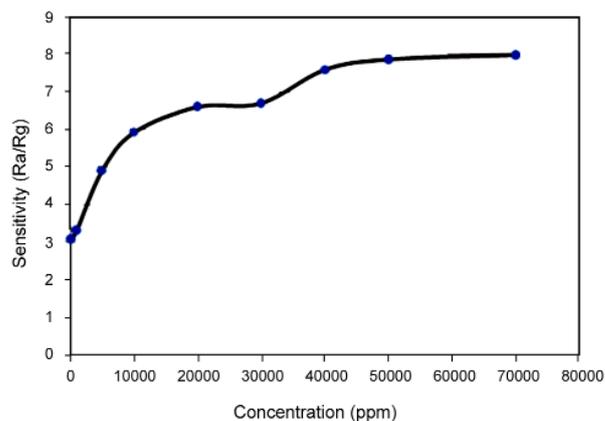
Mazhdi M et al

Int. J. Bio-Inorg. Hybd. Nanomat., Vol. 2, No. 1 (2013), 295-302
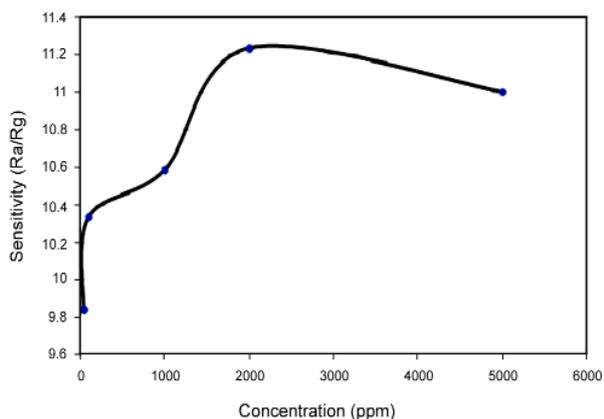
(a)
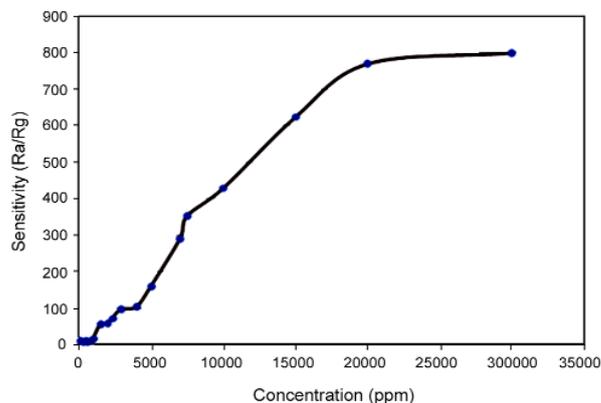
(a)

(b)

(b)

Figure 8: Sensor response (Sensitivity) to different concentration for ethanol vapor; ZnO (a), ZnO: Mn (b) nanocrystals.

Figure 9: Sensor response (Sensitivity) to different concentration for Gasoline vapor; ZnO (a), ZnO: Mn (b) nanocrystals.

Pure zinc oxide nanocrystals sensor will saturate in 2000 ppm of ethanol vapor whereas zinc oxide nanocrystals sensor doped by manganese achieves to saturation state in exceed of 70000 ppm. The doped sensor is able to sense the ethanol vapor by high concentration than pure one. By increase of ethanol vapor concentration, response and recovery times for pure sensor at first increase and then decrease and also are in order of 1 and 10 second respectively but for doped sensor response time decrease gradually and recovery time do not change tangible as for 1000 and 70000 ppm response and recovery times are 2, 12 and 2, 8 second respectively. Pure zinc oxide sensor in 30000 ppm

of gasoline vapor achieves to saturation state whereas doped zinc oxide sensor in 70000 ppm of gasoline vapor achieves to saturation state therefore doped zinc oxide sensor is a good choice for measurement of sample gas in high concentration. The results for sensor response to concentration show that response time of pure zinc oxide sensor to gasoline vapor decrease and recovery time increase regularly that are in order of 10 and 1000 second respectively. For 1000 and 30000 ppm of gasoline vapor, response and recovery times are 240, 6630 and 5, 20000 second respectively. By increase of gasoline vapor concentration, doped sensor response time decrease and its recovery time

Int. J. Bio-Inorg. Hybd. Nanomat., Vol. 2, No. 1 (2013), 295-302

Mazhdi M et al

increase respectively, as for 1000 and 70000 ppm of gasoline vapor, response and recovery times are 19, 70 and 5, 171 second respectively.

4. CONCLUSIONS

ZnO and ZnO: Mn nanocrystals with hexagonal structure were synthesized by the reverse micelle method using PVP as surfactant. The XRD studies of these nanocrystals revealed that the average particle size is about 21 and 18 nm for ZnO and ZnO: Mn nanocrystals, respectively. The atomic absorption studies confirmed attendance of manganese at zinc sites in ZnO: Mn nanocrystals. Sensor devices were fabricated and their gas sensing properties with respect to gasoline and ethanol vapor at different concentrations were measured. Gas sensing properties of these sensors showed that those are sensitive to both gasoline and ethanol vapors. Optimum working temperature to ethanol vapor for pure and doped zinc oxide nanocrystals sample was 362°C and 345°C and also for gasoline vapor was 285°C and 333°C respectively. Pure zinc oxide sensor achieve to saturation state at 2000 ppm and 30000 ppm for ethanol and gasoline vapor, respectively. Doped zinc oxide sensor for both gas sample (i.e. ethanol and gasoline) in 70000 ppm achieve to saturation state. Further studies showed that Mn doped ZnO nanoparticles based sensors have faster response and recovery time and the sensor will be saturated at higher concentrations.

REFERENCES

1. Maensiri S., Masingboon C., Promarak V., Seraphin S., *Opt. Mater.*, **29**(2007), 1700.

2. Mazhdi M., Hossein Khani P., Chitsazan Moghadam M., *IJND*, **2**(2011), 117.

3. Mazhdi M., Hossein Khani P., *IJND*, **2**(2012), 233.

4. Jayakumar O.D., Gopalakrishnan I.K., Kadam R.M., Vinu A., Asthana A., Tyagi A.K., *J. Cryst. Growth*, **300**(2007), 358.

5. Xu C., Tamaki J., Miura N., Yamazor N., *Sens. Actuators B*, **3**(1991), 147.

6. Khorsand Z., Abd. Majid W.H., Abrishami M.E., Yousefi R., *Solid-State Sci.*, **13**(2011), 251.

7. Mohamadrezaei A., Afzalzadeh R., *Sensor Lett.*, **8**(2010), 777.

8. Tan O.K., Cao W., Hu Y., Zhu W., *Ceram. Int.*, **30**(2004), 1127.

9. Takata M., Tsubone D., Yanagida H., *J. Am. Ceram. Soc.*, **59**(1976), 4.